

Appendix for

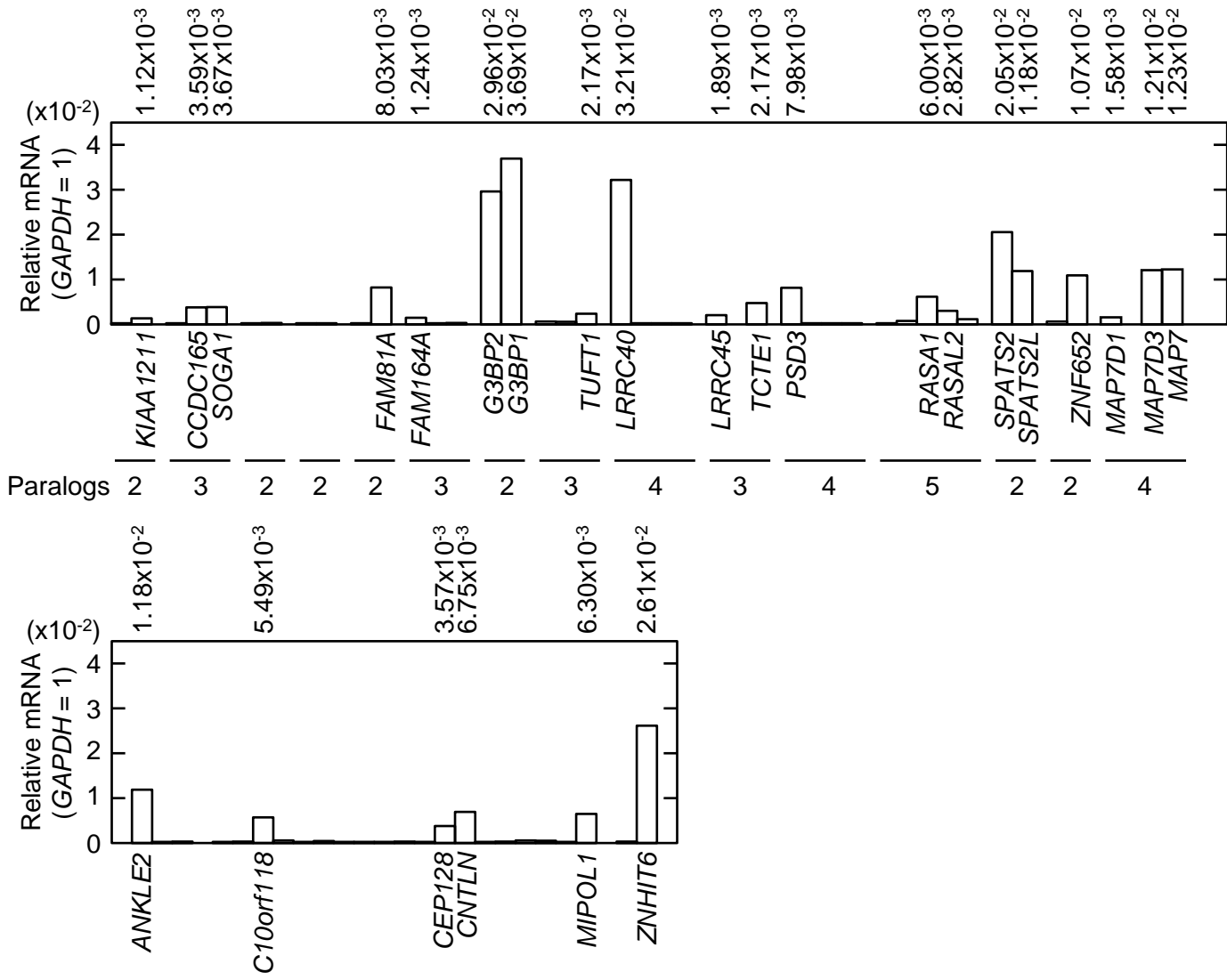
Map7/7D1 and Dvl form a feedback loop that facilitates microtubule remodeling and Wnt5a signaling.

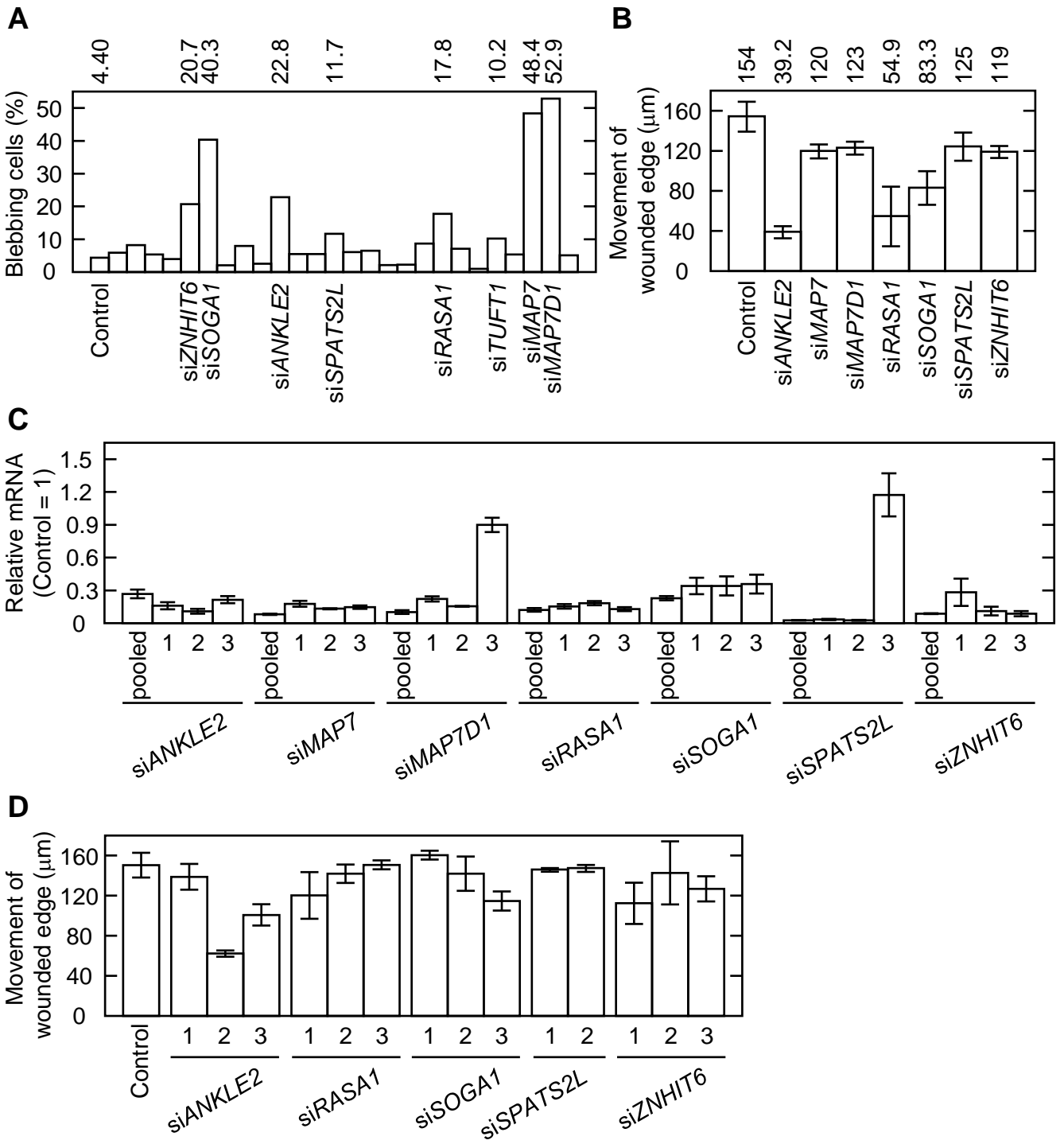
Koji Kikuchi^{1*}, Akira Nakamura^{2, 3}, Masaki Arata⁴, Dongbo Shi⁵, Mami Nakagawa⁵, Tsubasa Tanaka^{2, 3}, Tadashi Uemura⁴, Toshihiko Fujimori⁵, Akira Kikuchi⁶, Akiyoshi Uezu¹, Yasuhisa Sakamoto¹, and Hiroyuki Nakanishi^{1*}

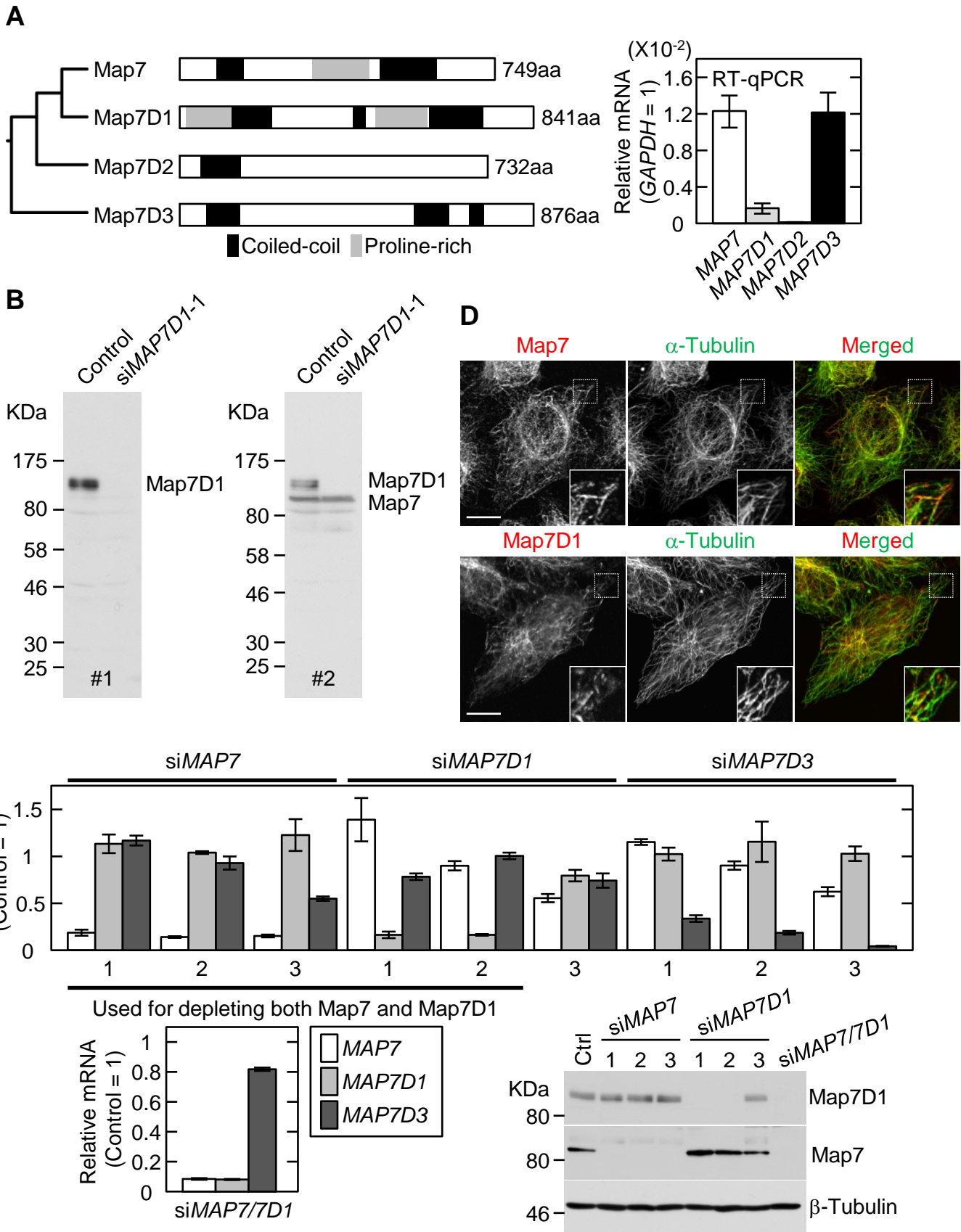
Table of content

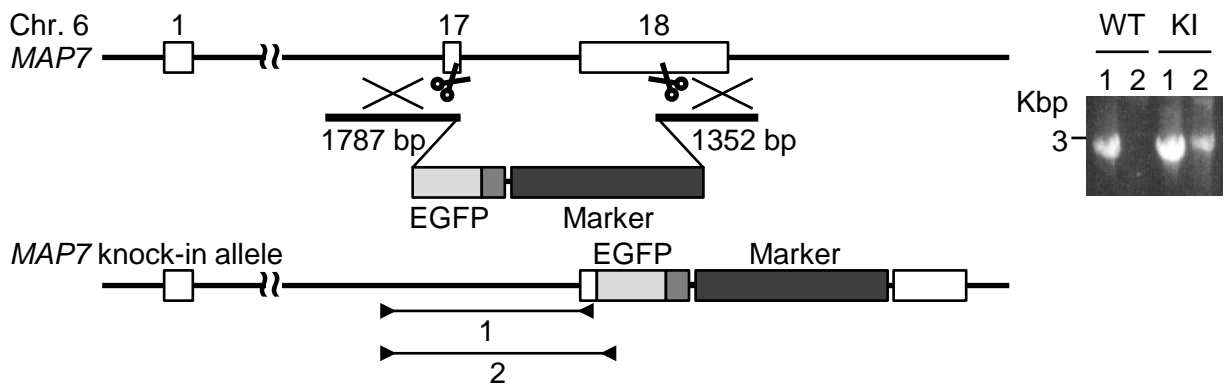
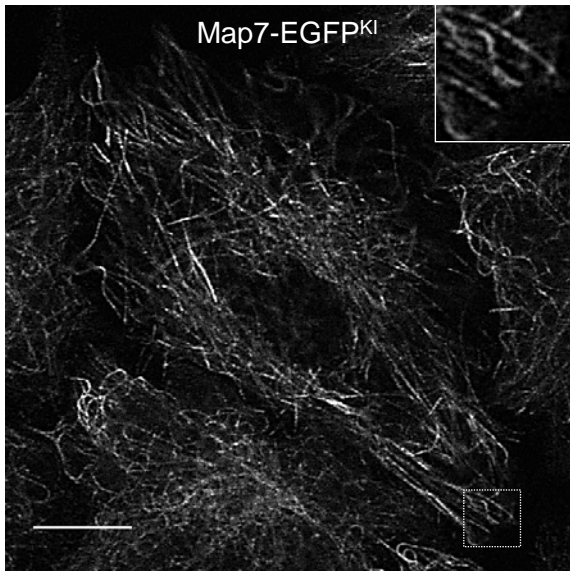
Appendix Figure S1.	Expression levels of candidate genes in HeLa cells.	3
Appendix Figure S2.	siRNA-based screen in HeLa cells to discover MT-binding protein(s) potentially involved in the Wnt/PCP signaling pathway.	4
Appendix Figure S3.	Map7 and its paralog, Map7D1 belong to the MAP7 family.	5
Appendix Figure S4.	Generation of Map7-EGFP knock-in HeLa cells.	6
Appendix Figure S5.	Phenotypes of Map7/7D1-depleted HeLa cells.	7
Appendix Figure S6.	Specific complex formation between Map7/7D1 and Dvl.	8
Appendix Figure S7.	Generation of Dvl2-EGFP knock-in HeLa cells.	9
Appendix Figure S8.	Wnt5a signaling and the Kinesin-1 member Kif5b promote directional Map7 movement toward the MT plus-end.	10
Appendix Figure S9.	Generation of <i>Ens::EGFP</i> knock-in fly strains.	11
Appendix Figure S10.	Generation of <i>ens</i> null mutants.	12
Appendix Figure legends		13-18
Appendix Table S1.	Primary antibodies used in this study.	19
Appendix Table S2.	siRNAs used in this study except for the siRNA-based screen.	20

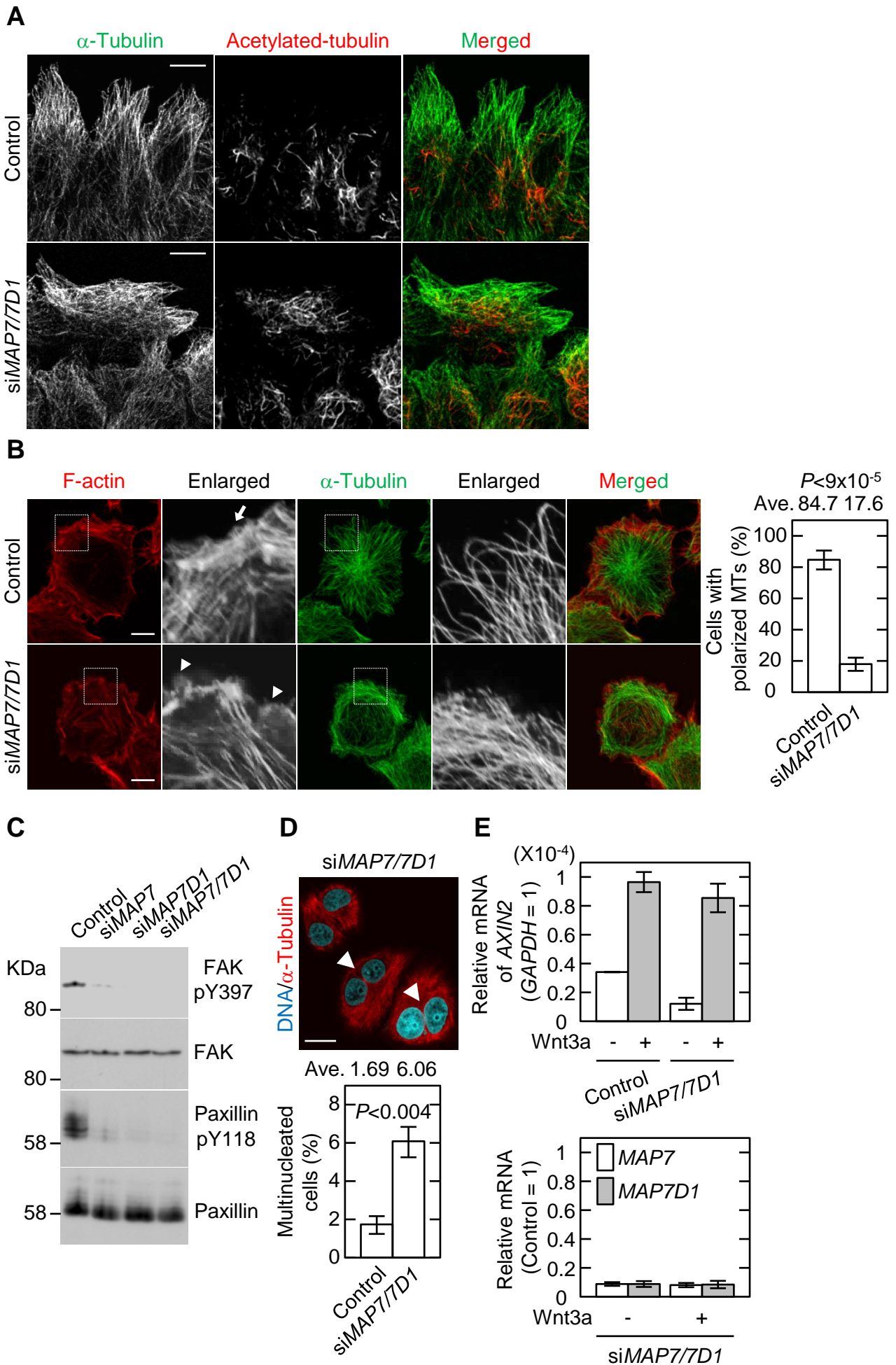
Appendix Table S3.	sgRNA sequences used in this study.	20
Appendix Table S4.	Primer sequences for RT-qPCR used in this study.	21-24
Appendix Table S5.	siRNA sequences for the siRNA-based screen used in this study.	25-26
Appendix Table S6.	Fly strains used in this study.	27
Appendix References		28

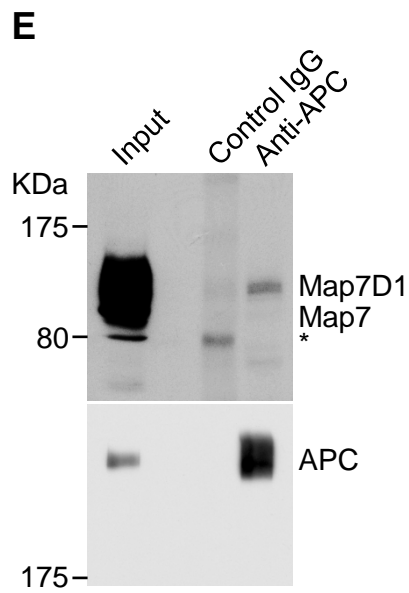
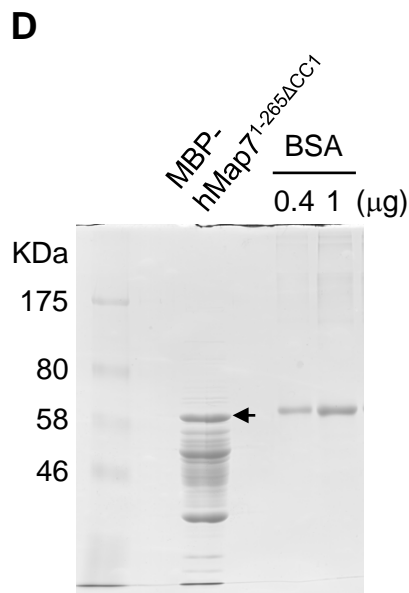
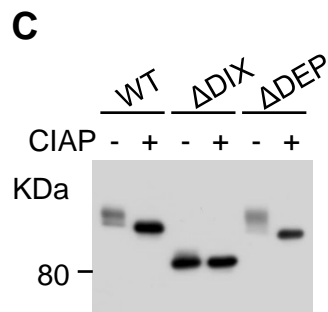
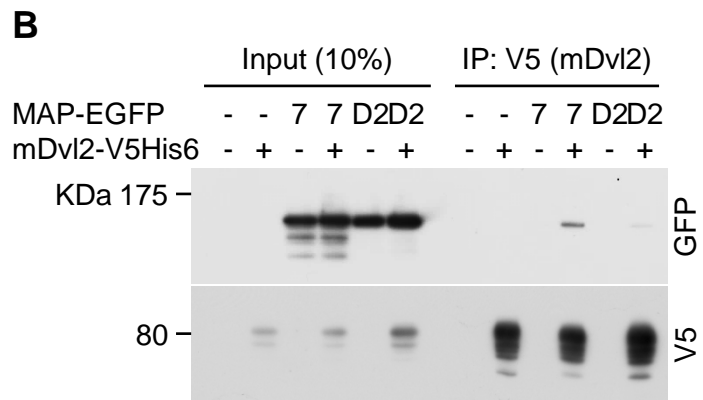
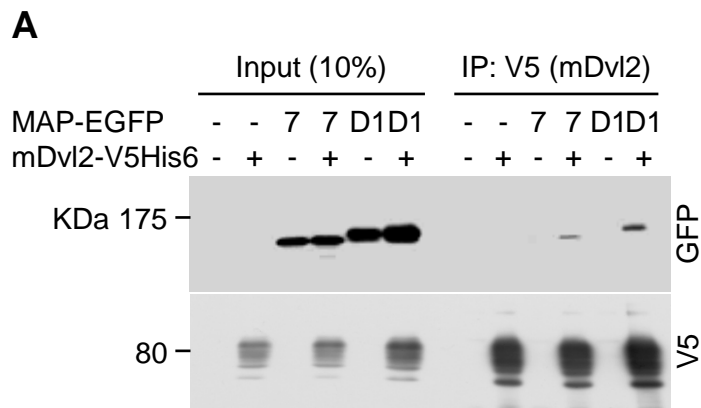


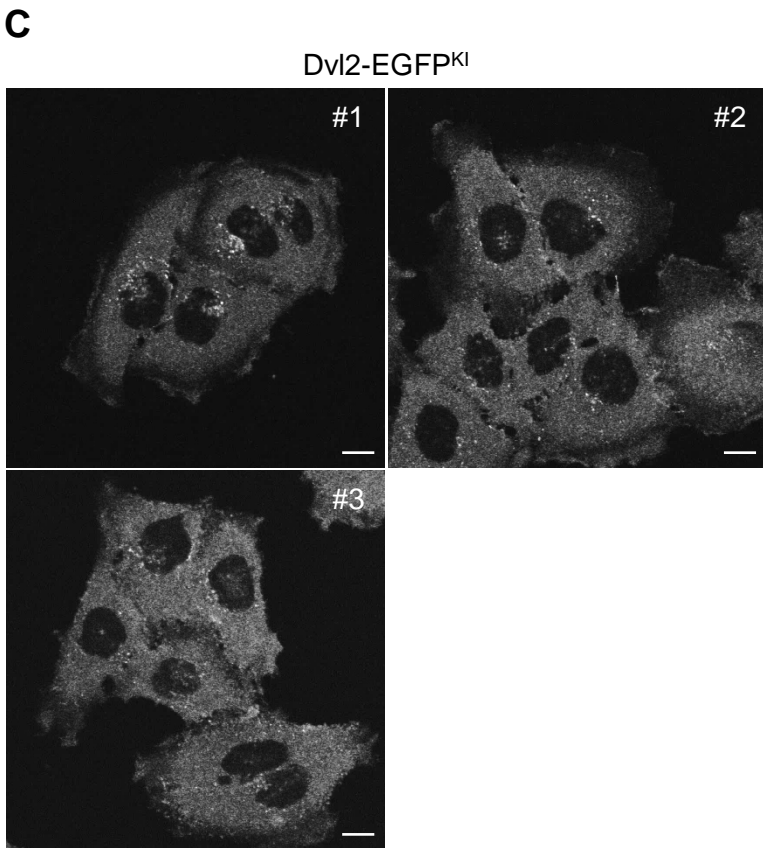
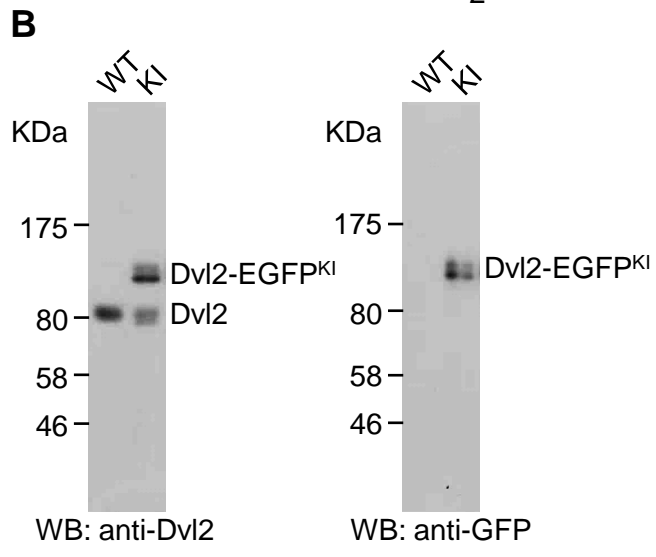
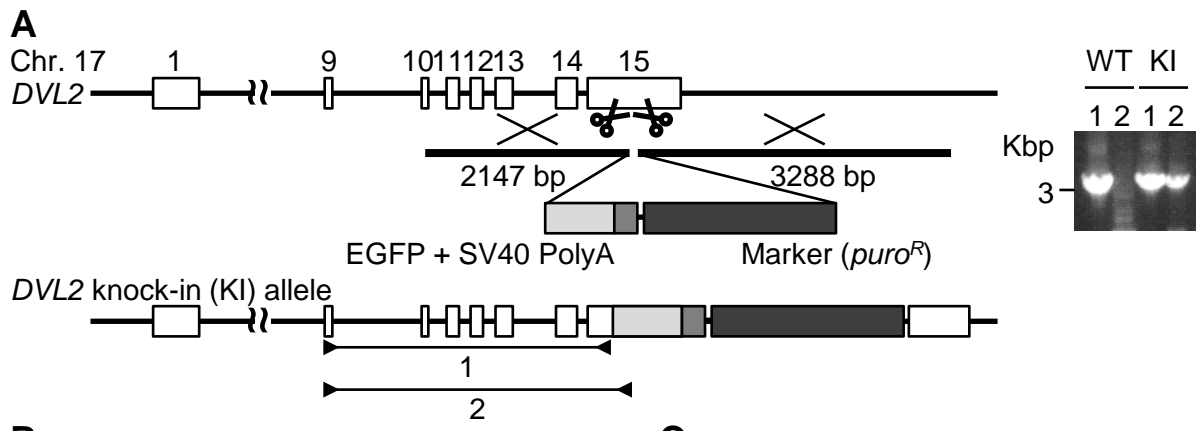


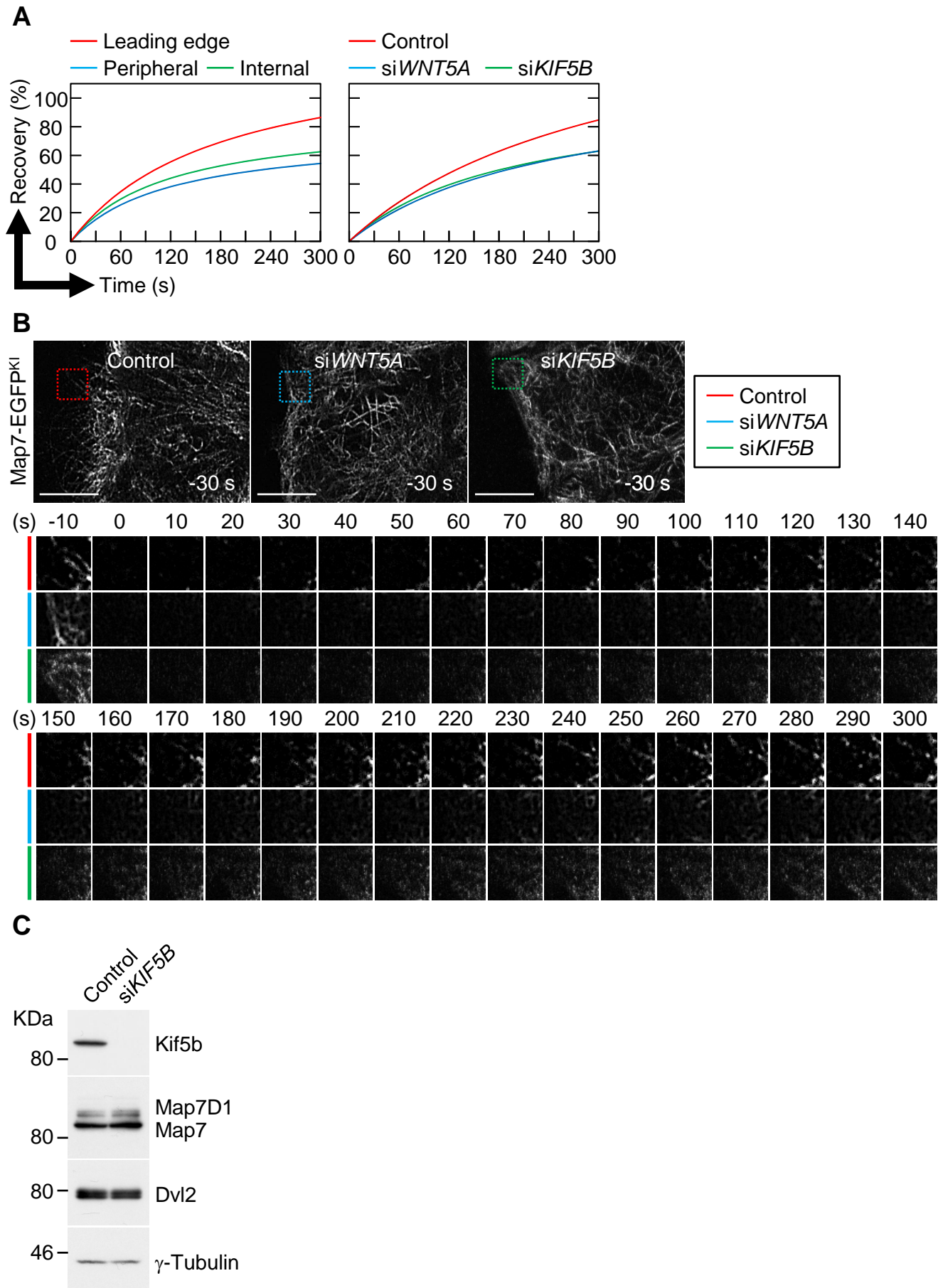


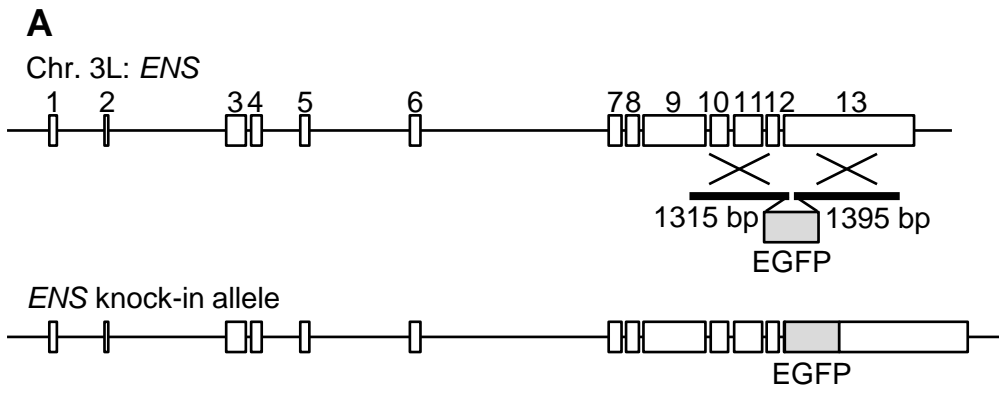
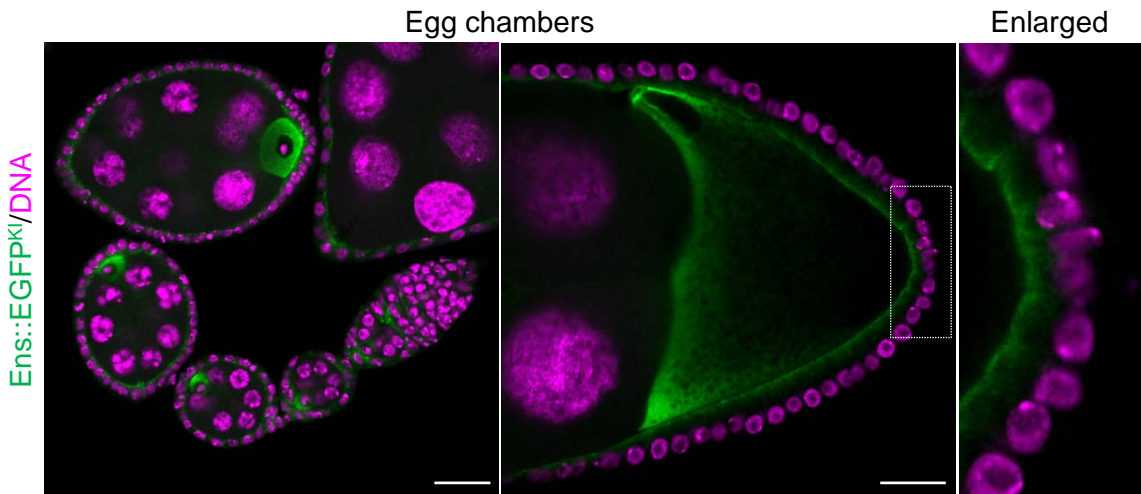
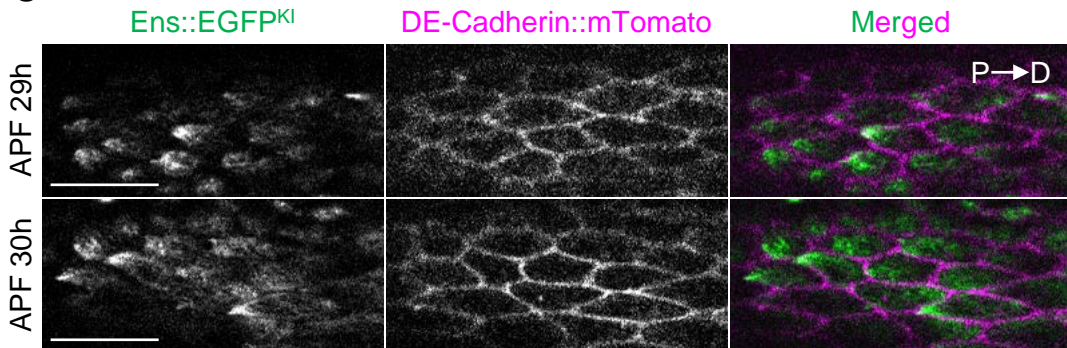
A**B**









**B****C**

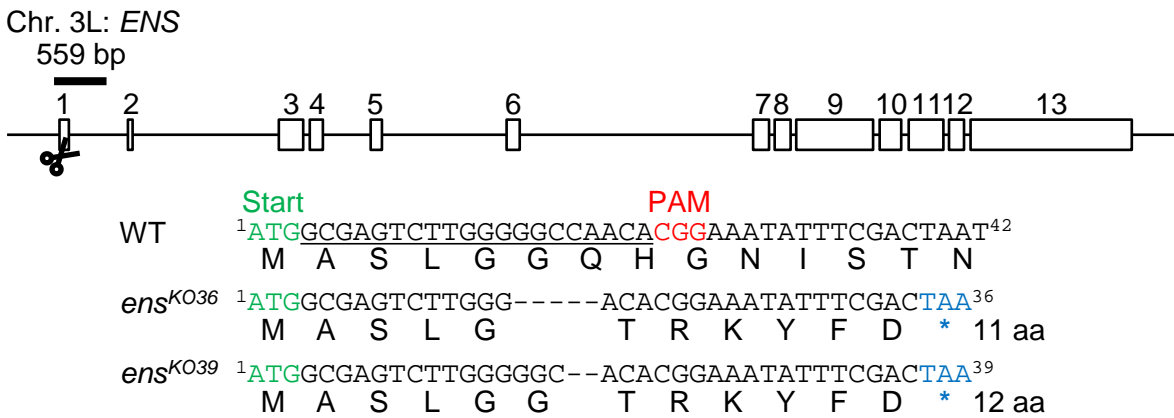
A

Female: <i>Df(3L)ens^{Δ3277}</i>		Hemizygous	Heterozygous	Mendelian inheritance	Lethality (%)
Male:	<i>ens^{KO36}</i>	82	703	351.5	76.7
	<i>ens^{KO39}</i>	43	682	341	87.4
	<i>ens^{ΔC}</i>	46	412	206	77.7

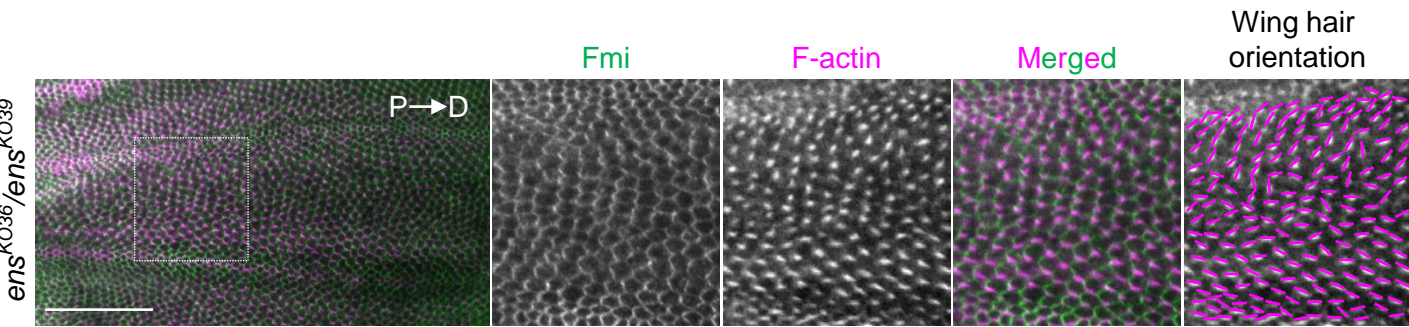
	Homozygous	Heterozygous	Mendelian inheritance	Lethality (%)
<i>ens^{KO36}</i>	2	1091	545.5	99.6
<i>ens^{KO39}</i>	0	559	144.5	100
<i>ens^{ΔC}</i>	98	271	135.5	27.7

Female	Male	Trans-heterozygous	Heterozygous	Mendelian inheritance	Lethality (%)
<i>ens^{KO36}</i>	<i>ens^{KO39}</i>	0	501	250.5	100
<i>ens^{KO39}</i>	<i>ens^{KO36}</i>	0	562	281	100

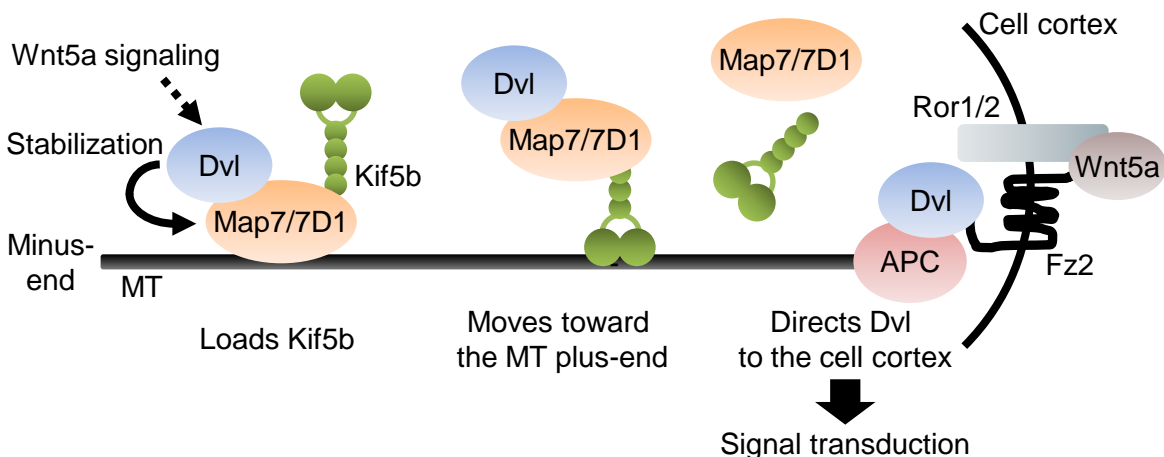
B



C



D



Appendix Figure legends

Appendix Figure S1. Expression levels of candidate genes in HeLa cells.

The expression levels of 69 genes for uncharacterized MT co-sedimented proteins and their paralogs were analyzed in HeLa cells by RT-qPCR. The relative mRNA level of each gene was normalized to the *GAPDH* expression. The primer list is shown in Appendix Table S4. Data are from two independent experiments and represent the average.

Appendix Figure S2. siRNA-based screen in HeLa cells to discover MT-binding protein(s) potentially involved in the Wnt/PCP signaling pathway.

A. Primary screening by cell spreading assays using siRNA pools for the indicated genes. Data represent the percentage of blebbing cells 60 min after being replated on a fibronectin-coated glass-bottom dish (total number of blebbing cells divided by total cell number, from four independent experiments). The siRNA list is shown in Appendix Table S5.

B. Wound healing assay using siRNA pools for the indicated genes. Data are from four independent experiments and represent the average distance moved by the wounded edge 6 h after wounding, \pm S.D.

C. RT-qPCR analysis for the depletion efficiency of the indicated siRNAs. At 72 h post-transfection with control or the indicated siRNAs, the mRNA level of each gene was quantified and normalized to the *GAPDH* expression. The mRNA level relative to that of control cells is shown. Data are from three independent experiments and represent the average \pm S.D.

D. Wound healing assay of cells transfected with each validated siRNA individually. Data are from three independent experiments and represent the average distance moved by the wounded edge 6 h after wounding, \pm S.D.

Appendix Figure S3. Map7 and its paralog, Map7D1 belong to the MAP7 family.

A. Schematic structures of MAP7 family proteins (left). Expression levels of MAP7 family genes in HeLa cells. The mRNA level of each gene normalized to the *GAPDH* expression is shown.

B. Specificity of anti-Map7D1 antibodies was evaluated by immunoblotting. HeLa cells were transfected with the indicated siRNAs. To detect Map7D1 alone, we used antibody #1, which hardly recognized Map7. Because antibody #2 recognized both Map7D1 and Map7, we used #2 to detect both of these proteins.

C. Specificity of siRNAs against Map7, Map7D1, or Map7D3. At 72 h post-transfection with control or the indicated siRNAs, cells were lysed, and the expression levels of *MAP7*, *MAP7D1*, and *MAP7D3* were quantified by normalization to the *GAPDH* expression. Relative mRNA levels to control cells are shown. In addition, specificity of siRNAs against Map7 or Map7D1 was confirmed by immunoblotting (the right of the bottom panel). The double depletion of Map7 and Map7D1 was achieved by transfecting cells with a mixture of three validated siRNAs against Map7 and the two against Map7D1.

D. Subcellular localization of endogenous Map7 or Map7D1 in non-migrating HeLa cells. To see the co-localization of MTs, fixed cells were co-immunostained for α -tubulin. Scale bars, 10 μ m.

Data information: Data are from three independent experiments and represent the average \pm S.D in A and C.

Appendix Figure S4. Generation of Map7-EGFP knock-in HeLa cells.

A. Schematic representation of the strategy to generate Map7-EGFP knock-in (Map7-EGFP^{KI}) HeLa cells by the CRISPR-Cas9 technique (left). The knock-in (KI) was confirmed by PCR using genomic DNAs derived from parental HeLa cells (WT) or Map7-EGFP^{KI} HeLa cells (KI) as a template. The positions of primer sets detecting the control (1) or KI (2) allele are shown at the right panel.

B. An image of the Map7-EGFP^{KI} localization in living cells (see Movie EV1). Scale bars, 10 μ m.

Appendix Figure S5. Phenotypes of Map7/7D1-depleted HeLa cells.

A. Control and Map7/7D1-depleted migrating cells stained for acetylated-tubulin. Cells were fixed 1 h after wounding, and stained with anti- α -tubulin (green) and anti-acetylated-tubulin (red) antibodies.

B. Peripheral MTs in the indicated cells during cell adhesion. Cells were fixed 1 h after being replated on fibronectin-coated cover glass, and stained with an anti- α -tubulin antibody and Phalloidin. Map7D/7D1 depletion caused a decrease in the proportion of cells with polarized MT arrays that were induced by cell adhesion. Cells with Map7/7D1-depletion failed to form lamellipodia (arrow), and instead exhibited membrane blebbing (arrowheads). Graph shows the percentage of cells with polarized MT arrays.

C. Kinetics of FA turnover during cell adhesion was evaluated in the indicated cells by measuring the cell adhesion-dependent activation of FAK. Cells were lysed 1 h after being replated on a fibronectin-coated dish. Map7/7D1-depleted cells exhibited decreased auto-phosphorylation of FAK on Tyr397 (pY397) and FAK-dependent phosphorylation of Paxillin on Tyr118 (pY118) during cell adhesion.

D. Image of multinucleated cells induced by depleting Map7/7D1. Cells were stained with DAPI (DNA) and an anti- α -tubulin antibody. Graph shows the percentage of multinucleated cells in the indicated cell types.

E. The Wnt3a-induced expression of *AXIN2* in the indicated cells. Cells were lysed 8 h after addition of buffer or purified Wnt3a (20 ng/ml). Expression level of *AXIN2* transcripts was quantified by normalization to the *GAPDH* expression at the top panel. Depletion efficiency of Map7/7D1 was shown at the bottom panel.

Data information: Scale bars, 10 μ m in A, B, and D. Data are from three independent experiments and represent the average \pm S.D in B, D, and E. Statistical significance was tested with the Student's *t*-test in B and D.

Appendix Figure S6. Specific complex formation between Map7/7D1 and Dvl.

A. Lysates from HeLa cells co-expressing hMap7-EGFP or mMap7D1-EGFP with mDvl2-V5His₆ were immunoprecipitated with an anti-V5 antibody, and the immunoprecipitates were probed with anti-GFP and anti-V5 antibodies.

B. Lysates from HeLa cells co-expressing hMap7-EGFP or rat (r) Map7D2-EGFP with mDvl2-V5His₆ were immunoprecipitated with an anti-V5 antibody, and the immunoprecipitates were probed with anti-GFP and anti-V5 antibodies.

C. The phosphorylation state of the indicated Dvl2 mutants. Lysates from HeLa cells expressing various mutants of mDvl2-EGFP were immunoprecipitated with an anti-GFP antibody, and the immunoprecipitates were treated with (+) or without (-) alkaline phosphatase (CIAP).

D. The amount of MBP-hMap7^{1-265ΔCC1} was determined on SDS polyacrylamide gels with Coomassie brilliant blue staining. Arrow shows the intact MBP-hMap7^{1-265ΔCC1}.

E. Lysates from HeLa cells were subjected to immunoprecipitation with control IgG or an anti-APC antibody, and analyzed by immunoblotting with an anti-Map7/7D1 or anti-APC antibody.

Appendix Figure S7. Generation of Dvl2-EGFP knock-in HeLa cells.

A. Schematic representation of Dvl2-EGFP knock-in (Dvl2-EGFP^{KI}) HeLa cell generation by the CRISPR-Cas9 technique. The KI was confirmed by PCR using genomic DNA derived from parental HeLa cells (WT) or Dvl2-EGFP^{KI} HeLa cells (KI) as a template (right panel). The positions of the primer sets for detecting the control (1) or KI (2) allele are shown at the bottom of the left panel.

B. Dvl2-EGFP^{KI} expression was confirmed by immunoblotting. Lysates derived from the indicated cells were probed with anti-Dvl2 (left panel) and anti-GFP (right panel) antibodies. The number of KI events on the pseudo-triploid HeLa genome was estimated by comparing the band intensity of Dvl2 with that of Dvl2-EGFP^{KI}. In this experiment, a cell strain in which EGFP was inserted into two of the three *Dvl2* loci was used.

C. Localization patterns of Dvl2-EGFP^{KI} in three independent clones. The same localization pattern was seen in all of the clones. Scale bars, 10 μm.

Appendix Figure S8. Wnt5a signaling and the Kinesin-1 member Kif5b promote directional Map7 movement toward the MT plus-end.

A. Graph shows fitted curves from the indicated data sets, related to Fig. 7.

B. FRAP analysis of Map7-EGFP^{KI} at the leading edge of the indicated cells after wounding. Cropped images of Map7-EGFP^{KI} at the leading edge of the indicated cells after wounding, related to Fig. 7B.

C. Confirmation of the depletion efficiency of si*KIF5B*. Lysates derived from the indicated cells were separated by SDS-PAGE, and immunoblotted for Kif5b, Map7/7D1, and Dvl2. Kif5b depletion did not affect the expression of Map7/7D1 or Dvl. The blot was reprobbed for γ -tubulin as a loading control.

Appendix Figure S9. Generation of Ens::EGFP knock-in fly strains.

A. Schematic representation of the generation of an Ens::EGFP knock-in (Ens::EGFP^{KI}) fly by the CRISPR-Cas9 technique.

B. Images of Ens::EGFP^{KI} egg chambers. Egg chambers were counterstained with DAPI (DNA). Enlarged image shows the Ens::EGFP^{KI} localization to the apical region in the follicle cell epithelium.

C. Single channel images for live pupal wings in Ens::EGFP^{KI} pupae expressing DE-Cadherin::mTomato at 29 and 30 h APF. P, proximal side; D, distal side.

Data information: Scale bars, 10 μ m in B and D

Appendix Figure S10. Generation of *ens* null mutants.

A. Lethality of different *ens* mutants. A few *ens*^{KO} *neoFRT80B/Df(3L)ens*^{A3277} hemizygous escapers were eclosed, all of which died immediately after eclosion. In addition, *ens*^{KO} *neoFRT80B/ens*^{KO}

neoFRT80B homozygous or transheterozygous mutants died before eclosion. In contrast, *ens^{AC} neoFRT80B/Df(3L)ens^{A3277}* hemizygous mutants survived up to two weeks after eclosion, and increased numbers of *ens^{AC} neoFRT80B/ens^{AC} neoFRT80B* homozygous mutants were eclosed, suggesting that the remaining N-terminal portion encoded by the *ens^{AC}* allele allowed the organisms to grow to the adult stage.

B. Schematic representation of the generation of *ens* null mutants by the CRISPR-Cas9 technique. The deletions in the two *ens* null alleles are shown.

C. Pupal wings of *ens^{KO36}/ens^{KO39}* mutants at 32-34 h APF were stained with an anti-Fmi antibody and Phalloidin. P, proximal side; D, distal side. High magnification views of boxed area (intervein region between L3 and L4 veins) are shown at right. Magenta lines in right side panels indicate wing hair orientation. Because *ens^{KO36}/ens^{KO39}* mutants died before eclosion, we obtained their pupae by selecting third instar larvae, which were identified by the loss of GFP fluorescence from the balancer chromosome. Note that defects in wing hair orientation in *ens^{KO36}/ens^{KO39}* pupae were virtually identical to those in wing hair orientation in *ens^{KO36}/Df(3L)BSC735* pupae. Therefore, off-target mutations in *ens^{KO36}* or *ens^{KO39}* chromosomes should not affect planar cell polarity on wing epithelium. Scale bar, 10 μ m.

D. Proposed model for the actions of Map7/7D1 in Wnt5a signaling. See Discussion in detail.

Appendix Table S1. Primary antibodies used in this study.

Company	Name, catalog number	Used for (dilutions)
Absea	Rat anti-APC (KT45), 030903E07	IF (1:200)
Bioresource	Rabbit anti-FAK pY397, 44-624G	IB (1:3000)
BD Biosciences	Mouse anti-Clathrin heavy chain, 610500	IB (1:5000)
	Mouse anti-FAK, 610088	IB (1:3000), IF (1:250)
	Mouse anti-EB1, 610535	IF (1/500)
	Mouse anti-Paxillin, 610052	IB (1:3000), IF (1:250)
Chromotek	Rat anti-RFP, 6g6-100	IF (1:200)
Cell Signaling Technology	Rabbit anti-Dvl2, 3216	IB (1:3000), IP
	Rabbit anti-Paxillin pY118, 2541	IB (1:3000)
	Rabbit anti-Wnt5a/b, 2530	IB (1:1500)
DSHB*	Mouse anti-Fmi, #74	IF (1:20)
	Rabbit anti-Kinesin (Kif5b), GTX104874	IB (1:3000)
GeneTex	Mouse anti-GFP, M048-3	IB (1:2000)
	Mouse anti-MBP, M091-3	IB (1:3000)
MBL	Rabbit anti-GFP, 598	IB (1:5000), IF (HeLa, 1:500; Fly, 1:200), IP
	Rabbit anti-GST, PM013	IB (1:3000)
	Rabbit anti-Detyrosinated tubulin, AB3201	IB (1:3000)
	Mouse anti-V5, 04434-36	IB (1:3000), IP
Nacalai	Rat anti-GFP, 04404-84	IF (HeLa, 1:500)
	Goat anti-Fz6, AF1526	IF (1:100)
R&D systems	Rabbit anti-APC (C-20), sc-896	IB (1:1500), IP
Santa Cruz Biotechnology	Mouse anti-Acetylated tubulin, T7451	IB (1:5000), IF (1:500)
	Mouse anti- α -tubulin (DM1A), T6199	IF (1:1000)
	Mouse anti- β -tubulin, T0198	IB (1:5000)
	Mouse anti- γ -tubulin (GTU-88), T6557	IB (1:5000)
	Rabbit anti-Flag, F7425	IF (1:500)
	Rabbit anti-Map7, SAB1408648	IB (1:3000), IF (1:250)
	Rabbit anti-Map7D1#1	IB (1:5000), IF (1:500)
Sigma-Aldrich	Mouse anti- α -tubulin (DM1A), T6199	IF (1:1000)
	Mouse anti- β -tubulin, T0198	IB (1:5000)
T. Fujimori's lab	Mouse anti- γ -tubulin (GTU-88), T6557	IB (1:5000)
	Rabbit anti-Map7, SAB1408648	IB (1:3000), IF (1:250)
	Rabbit anti-Map7D1#1	IB (1:5000), IF (1:500)
Made in-house	Guinea pig anti-Celsr1 [1]	IF (1/100)
	Rat anti-E-cadherin [2]	IF (1/2)
Made in-house	Rabbit anti-Map7D1#1	IB (1:5000), IF (1:500)
	Rabbit anti-Map7D1#2	IB (1:5000)

IB, Immunoblotting; IF, Immunofluorescence; IP, Immunoprecipitation

*, The Developmental Studies Hybridoma Bank

Appendix Table S2. siRNAs used in this study except for the siRNA-based screen.

Name	Sequence (sense)
Randomized control [3]	5'-CAGUCGCGUUUGCGACUGGTT-3'
<i>MAP7</i> 3' UTR-1	5'-AUUAAUUGUAGAAAUUCUCAU-3'
<i>MAP7</i> 3' UTR-2	5'-UAUUUGAUUAGUUUAUCUGGA-3'
<i>DVL1</i> [3]	5'-GGAGGAGAUCUUUGAUGACTT-3'
<i>DVL2</i> [3]	5'-GGAAGAAAUUUCAGAUGACTT-3'
<i>DVL3</i> [3]	5'-GGAGGAGAUCUCGGAUGACTT-3'
<i>WNT5A</i> [3]	5'-GUUCAGAUGUCAGAAGUAUTT-3'
<i>APC</i> [3]	5'-GAGCGGCAGAAUGAAGGUCAA-3'
<i>KIF5B-1</i> [4]	5'-GCAAGAAGUAGAUCGCAUATT-3'
<i>KIF5B-2</i> [4]	5'-GCUGUCAAUUAUGAUCAGATT-3'
<i>KIF5B-3</i> [4]	5'-GACAUGUAGCAGUUACAAATT-3'

Appendix Table S3. sgRNA sequences used in this study.

Name	Sequence (sense)
<i>MAP7_KI-1</i>	5'-G TTCAGACACAGCAGACTGC-3'
<i>MAP7_KI-2</i>	5'-G TTGACTGTGTTTGGCACAC-3'
<i>DVL2_KI-1</i>	5'-CAATCCCAGCGAGTTCTTTG-3'
<i>DVL2_KI-2</i>	5'-GTGCTTGCTCTTACAGTGCC-3'
<i>ens_KO-1</i>	5'-GCGAGTCTTGGGGGCCAACA-3'
<i>ens_KO-2</i>	5'-GGACCTCCGCTGACCCCAA-3'
<i>ens_KI-1</i>	5'-ACTATCAGCAGTGACTAGCG-3'
<i>ens_KI-2</i>	5'-ACGATCCCCGATCTCTGAGG-3'

Appendix Table S4. Primer sequences for RT-qPCR used in this study.

Primer name	Sequences
C2orf55+	TCCCGGATGAGGAGAAGG
C2orf55-	GTGTTTCAGGCAGCTCTTG
KIAA1211+	CAGTCCAGCACGCCCTA
KIAA1211-	CGTGCTTCTTCTCCTCCAA
C6orf174+	ACTGAGGCAACAGCTCATA
C6orf174-	TCATTGTCCTCCTCTGTGG
CCDC165+	TGAAACACTGGCGGCAA
CCDC165-	CCCACTGGAAAGCCACA
SOGA1+	CTAAGGAGATTCTTCTGGCAA
SOGA1-	CATTGTCTTCAGCTCGGTA
CCDC9+	CCCTGGAGGAGTCTGAG
CCDC9-	TGCTTCCAGCGCAGGTA
C15orf52+	AGGAGCCACCAGAAACT
C15orf52-	TCCTTCATATCCCACCTTCG
CCDC38+	TCCTCAGGGAGTATATGAAATATGG
CCDC38-	GATGCCTTCTTGTACTTGAAT
CCDC37+	TTGAAGACACTCTGAAGCATTAC
CCDC37-	CTGGTGTGGAGTTAACTG
FAM81B+	CGGCCACAGGAACTAAC
FAM81B-	TCTCAATTTGCCGGTGC
FAM81A+	TTGAACAAAGAACAGCAGGC
FAM81A-	TGGTGGTTACTGTCTCTGTGA
FAM164A+	GGATCTTCACGATTACCGC
FAM164A-	GTGGTGTGGAATTTCCGGG
FAM164B+	CGATCAGCAAAGCAGTGT
FAM164B-	TGCAGAAATTAGTATGTCGCTC
FAM164C+	CAGAAGGATCCAGACGC
FAM164C-	ATCCTCTCTCCTGTCTCTACTAA
G3BP2+	ACCAGAAGTTCAATCTCAGC
G3BP2-	TGATGACTATCTGGATAGCGAATTA
G3BP1+	GTGGAGCTGTTCCAGTTAC
G3BP1-	GGGAGGAATATTTATTCGTTGTTCT
GCOM1+	AGCCTAGAGGAGAAAGACC
GCOM1-	CTGATACCTTTCCTTGTCAGAAT
CCDC68+	TCTTAGAAATGAACAAAGAGAATGAAGTAT
CCDC68-	ACCTGGAGTAATTGTTTACTGTC
TUFT1+	GATGGAGACGGAGCATCA
TUFT1-	GTGGATCTTCTCCCGCA
LRR40+	TACGGTCCTTGAAAGGC
LRR40-	AGGACTTCTTGTGTTCTTTAC
LRR30+	CGAGGTCCAGAACTCAATC
LRR30-	CAGGCAGTTCATGTTGACAAA
LRRD1+	GTGCAATGTTGGAATGCC
LRRD1-	ATATGTTATTAAGATGTGAGATACAGTCAG

LRR1Q4+	TGACCTGGACGAGAACAAA
LRR1Q4-	GGAGGAGGTTGTGGGATAA
LRR45+	GCAGAGCGGGAGTCTAA
LRR45-	GCTGACATGCTGGTCATC
C14orf166B+	CTTCAAGGAAGACTCCGCA
C14orf166B-	GCTCAGATCCAGTGACG
TCTE1+	CAGCGAGGGAGAGATGG
TCTE1-	AAGGAGAGGCAGTCACG
PSD3+	TATACGGAGGACTCCACCGA
PSD3-	AATGCGCTGTTGTATCATTG
PSD+	TCCCTGCCACTCAGAGGA
PSD-	TGCCATTGGACAAGGT
PSD2+	GGGTCCTCACACACTTCTC
PSD2-	ATTGCTGACAGGACATCTTT
PSD4+	AGCTTCTTCTCCAGAGCCTA
PSD4-	AGTGAAGACTGTGAAGCATCTA
RASAL3+	GCTTCTACTGAGGACTGTGA
RASAL3-	AGCTTGAGAACACGATGC
DAB2IP+	GCTGGAGCAGAGCATAG
DAB2IP-	ATCGTTCTCAATCACCATCTT
RASA1+	GTTCTGTCTATGTCGTTTCATGAT
RASA1-	AAATGCCTGCAGACCTT
RASAL2+	GTTTCCCAACTTGATAAGGGT
RASAL2-	GGACTGGAGTTATGTTTCAGTG
SYNGAP1+	CATCGCAGACAGGCTTATC
SYNGAP1-	AAGTCCTCCTTTGAGGTAAC
SPATS2+	GCAGAATGGTGTCTCTGAT
SPATS2-	TTTACTGGTGGCGAGGG
SPATS2L+	AATTAAGCACTTTGTCAGCGA
SPATS2L-	CAGGGAGTTCTTGAGGAATAG
ZBTB47+	AGAAGAGGAAGAGGAAGGT
ZBTB47-	TGATCCTGCTCACTAGGC
ZNF652+	CTAAGCGTAAGAAGCGGG
ZNF652-	CAAATCTGCATGCGCCTA
MAP7D1+	GGACAAGGAGCGGGAAA
MAP7D1-	TGTGGAGGGAGAGGATGG
MAP7+	AACTCTTTGTAACACCACCT
MAP7-	GGTTGTCTTGCTTTGGGA
MAP7D2+	GGCATTCTAAGAGACCATC
MAP7D2-	CTTTCCTCTTGGGCATGT
MAP7D3+	CAAGTGTGGATGCACCC
MAP7D3-	TCCATGCTCATCTCAGAATCA
ANKLE2+	GTAAGTTTGGAAATGCAGATGTAG
ANKLE2-	CCTTTAAATACTCTCTGATCCGC
C1orf49+	TAAACAAGAAGGGCGGTTTAC
C1orf49-	TTCCTTCATAATTTCCACAAATTCG
C2orf16+	ACTATGGAAAGGAAGCTTTGT

C2orf16-	GGCTGAGAAATAGTAACTGGAC
C5orf49+	TCAGAAGTTGCACCGAGAT
C5orf49-	GCCAAAGTCCCGGTTTAG
C6orf97+	AAATCGCAGCCCTCCTTA
C6orf97-	TCCTTTCCCAACTGTTCAACAA
C10orf68+	GCAGTTAAAGAGAAAGAGTTACCC
C10orf68-	GGTTGACTCCTTCATTAGACC
C10orf118+	AAGGAAGGCGAAACGACTA
C10orf118-	TGTTGTTTCTTTGAGTTTATCTTTGG
C16orf45+	CAGAACTTGGTCGCCAT
C16orf45-	TTGTCTTCTTCTTGCTCCCT
CCDC13+	TTGTCTGTCTATCCAGACCC
CCDC13-	GTTCCGAGACCTCATGC
CCDC40+	CCATCATGAAGGAGGAAGAAA
CCDC40-	TGCAGGGTGAGCCTGTA
CCDC67+	ACTTGAATCATCTTATTTGCCTTCTATTA
CCDC67-	GATGAAGCTCTTCTGTTAGGTC
CCDC83+	CCAGGTATCCAGTGCTACA
CCDC83-	GCAATTCCAAAGACATTTCTTCAG
CCDC146+	GCTAAGAGGAATTTGGCCC
CCDC146-	CTTTCATTTCTTTAACAATGTTGGTGTA
CCDC147+	TCGAACAGCACAAAGAAACC
CCDC147-	CCGCCTTAAGCATGTTCTTAT
CEP112+	AACATGAAACTGTTACAAACCAAATA
CEP112-	GCTTTCTTTGAAGTTCTGATTCC
CEP128+	CTGTATGCAGCATTACAACAAATAG
CEP128-	AATTCTTAACTTCCAATTCAAGGTC
CNTLN+	TGTGGAATGAACTGGCATATTT
CNTLN-	GCTGTTCTTCTTCTCTCTG
CXorf58+	AGTCCAAAGTAACTGATATAATGGAT
CXorf58-	ACATTAGCATTGTCCTGGG
FHAD1+	ACAGAGTGAAGGAAGCATTAG
FHAD1-	GGGTAAATGGTTCTCCAGAT
FSIP1+	ATGAACTTGCAGTCACCC
FSIP1-	CCATATTTCTTTCACCATCACG
LOC100271840+	CTAATGAAGATGGAGTCCACG
LOC100271840-	GATCAGCGATGCCCTTG
LRRCC1+	CCTTGTTGAACAGCTAGACC
LRRCC1-	ATTTCCTTTAGCCTATCTGTGG
MIPOL1+	AGCAGAAATTGGCTAAAGAAGATAA
MIPOL1-	TAACAGCTTCATCACGTTCTT
RGSL1+	ACATGAAGGAAATGGACTATAGG
RGSL1-	GCCATCTTTGGGTTCTTGT
ZNF626+	CAAAGCCTTTAACCACTCTTG
ZNF626-	TAGGGTTTCTCTCCAGTATGATT
ZNHIT6+	GGAATTGATGCATGGAGAGT
ZNHIT6-	GCTTCTTCTGTACCACAAGT

GAPDH+	CCTGTTGACAGTCAGCCG
GAPDH-	CGACCAAATCCGTTGACTCC

Appendix Table S5. siRNA sequences for the siRNA-based screen used in this study.

NCBI gene symbol	siRNA Target Sequence
<i>G3BP1</i>	AACCCTGGTTCCAACAGAATG
<i>G3BP1</i>	CAGGAGGAGTCTGAAGAAGAA
<i>G3BP1</i>	CAGAAAGAAATCCACAGGAAA
<i>G3BP2</i>	AAGAGCTGCAAGAGAGCGAGA
<i>G3BP2</i>	CAGGGATATTAGGCGCAATGA
<i>G3BP2</i>	CCACCTCGTGTGCGTGAACAA
<i>C10orf118</i>	CAGCCTGTCATTGAATCTAAA
<i>C10orf118</i>	AAGGAAATTATTAATCGCCAA
<i>C10orf118</i>	ACACTACTTAACACTCCTAAA
<i>CEP128</i>	CAGGACCGTGTAAATTGCATTA
<i>CEP128</i>	AACGAGCGTTGGAGAAACAAT
<i>CEP128</i>	CACAGGGTATTAAACGAATGA
<i>ZNHIT6</i>	CACCGTCTAGCCACAGGAGAA
<i>ZNHIT6</i>	CACGTTGTATGCGATATTCCT
<i>ZNHIT6</i>	CTCCTAAGTGATTATCGATTT
<i>SOGA1</i>	TTCCTATGCCTCTGAGATCAA
<i>SOGA1</i>	CACGCCCAATGAGTACATCAA
<i>SOGA1</i>	ACGCTGTTTGTGACTGTAGTA
<i>ZC2HC1A</i>	CCCGAAATTCCACACCACCTA
<i>ZC2HC1A</i>	AACAGGCAGCACGTATTAGTA
<i>ZC2HC1A</i>	TGCCATGAGTGTGGACTAAA
<i>CNTLN</i>	CACAGCTGAAAGTATATCATA
<i>CNTLN</i>	AAGGAGTGTGTACAGAACAAA
<i>CNTLN</i>	CTGCACTGACCTGCTAAATGA
<i>FAM81A</i>	ATCCGTCAGAAGTATGATGTA
<i>FAM81A</i>	ACAGCCGTCTATGAAAGCATA
<i>FAM81A</i>	AAGGCTCAATATCTGCGTTGA
<i>ANKLE2</i>	ATCGTCAAAGCCGGATTGAAA
<i>ANKLE2</i>	CCGTTACGTGGTGGACCTGTA
<i>ANKLE2</i>	AAGGAGCGGATCAGAGAGTAT
<i>SOGA2</i>	ACCCACGAGCTCAGCAAGTTT
<i>SOGA2</i>	CCGACTCCTCCTGGTACCTAA
<i>SOGA2</i>	CTGCAGTACCGTCTTCGGAAA
<i>KIAA1211</i>	CAGGATCCACAACATGAGCAA
<i>KIAA1211</i>	ACCATCGAAAGTGTCAACTTA
<i>KIAA1211</i>	CAGCCGCTGTGGATAACGTTA
<i>SPATS2L</i>	CACCGTTTCTCTAACTAGATA
<i>SPATS2L</i>	TAGATATCGCGTCATGATTAA
<i>SPATS2L</i>	AAGATCTATGCAGTTAGATCA
<i>LRRC40</i>	AAGATGATGGACCTAGCCAAA
<i>LRRC40</i>	AAGGAATTGCACGTAGGTGAA
<i>LRRC40</i>	CAACATCGTCACTTCTATTAA
<i>LRRC45</i>	CTTGATGGAGACTATIGATAA

<i>LRRC45</i>	CTCCGAAAGCCTGCGCATCAA
<i>LRRC45</i>	CCGCACTCACGTCCTCAGCAA
<i>TCTE1</i>	CAAGACCCTCCTGGAATTTGA
<i>TCTE1</i>	CCCACCGTTGACCACTACCAA
<i>TCTE1</i>	CACAGCTCTCAAAGCCTTCAA
<i>MIPOL1</i>	ATGGGTAGCTATAAGGTTACA
<i>MIPOL1</i>	AACGGGATGCTGCCTTGTCTA
<i>MIPOL1</i>	CAGGGCAGAGATCAACGAATT
<i>PSD3</i>	AAGCGTGAAGATCGTAGGATT
<i>PSD3</i>	AAGGACGTGATGAGTACAAA
<i>PSD3</i>	CAGGGACTTCTGGATAGGCTA
<i>RASA1</i>	CAGCTCCCATATAACCATTA
<i>RASA1</i>	ACGGACCTGTCCCGTGATTTA
<i>RASA1</i>	CAGACCTAATAGGTTATTACA
<i>RASAL2</i>	CGGCGACTGGAGGAATATGAA
<i>RASAL2</i>	CTCGTGGGCTGCCTAAACTAA
<i>RASAL2</i>	AACCTTCGCAGGACAGTTCAA
<i>SPATS2</i>	TACGTGCAATAGTTCCTAATA
<i>SPATS2</i>	CACAGTGTCTCTTGACCGGTA
<i>SPATS2</i>	CGGTATCGAGTTGTAGTAAA
<i>TUFT1</i>	AAGTAGATAGGCATCAGAGTA
<i>TUFT1</i>	CTGAGGTGGACACCTGTATAA
<i>TUFT1</i>	CAGACGGAGCACGAGCACCTA
<i>ZNF652</i>	ACCAGCATTCTTAGGCGATAA
<i>ZNF652</i>	GCAGATCATAGTGGAGGTA
<i>ZNF652</i>	AGAGTGAGCCTTTAAATCATA
<i>MAP7</i>	CCTCTTCATCTGCAACTTT
<i>MAP7</i>	GGAGAGAAAGAAGCGACTT
<i>MAP7</i>	ATGAGAATTTCTACAATTA
<i>MAP7D1</i>	AGCGTCTGGAGGAGATCAT
<i>MAP7D1</i>	ATGAAGAGGACTCGGAAGT
<i>MAP7D1</i>	CCAAGGGGCGGGTTCGGAG
<i>MAP7D3</i>	AGCACTAACAGGCAAATCC
<i>MAP7D3</i>	GCTTTGAGCCAAAGGCATA
<i>MAP7D3</i>	GCCAATAAACGATCTGCAT

Appendix Table S6. Fly strains used in this study.

Used in	Genotype
Fig. 8C and Appendix Fig. S9C	<i>w; shg::mTomato; ens::EGFP^{K1}</i>
Fig. 9A	<i>Oregon-R</i>
Fig. 9A	<i>w; Df(3L)BSC735/TM6B P{Dfd-EYFP}3 Sb Tb ca</i>
Fig. 9A and Appendix Fig. S10C	<i>w; ens^{KO36} P{neoFRT}80B/TM6B P{Dfd-EYFP}3 Sb Tb ca</i>
Fig. 9C and Fig. EV2	<i>w; dsh::EGFP</i>
Fig. 9C and Fig. EV2	<i>w; dsh::EGFP; ens^{KO36} P{neoFRT}80B/TM3, P{sChFP}3 Sb</i>
Fig. 9C and Fig. EV2	<i>w; dsh::EGFP; ens^{KO39} P{neoFRT}80B/TM3, P{sChFP}3 Sb</i>
Appendix Fig. S9B	<i>w; ens::EGFP^{K1}</i>
Appendix Fig. S10A	<i>w; ens^{KO36} P{neoFRT}80B/TM3 Sb Ser</i>
Appendix Fig. S10A	<i>w; ens^{KO39} P{neoFRT}80B/TM3 Sb Ser</i>
Appendix Fig. S10A	<i>w; ens^{ΔC} P{neoFRT}80B/TM3 Sb Ser</i>
Appendix Fig. S10A	<i>w; Df(3L)ens^{Δ3277}, Chd64^{Δ3277} ens^{Δ3277} P{neoFRT}80B/TM3 Sb^l</i>
Appendix Fig. S10C	<i>w; ens^{KO39} P{neoFRT}80B/TM6B P{Dfd-EYFP}3 Sb Tb ca</i>

Appendix References

1. Shi D, Komatsu K, Hirao M, Toyooka Y, Koyama H, Tissir F, Goffinet AM, Uemura T, Fujimori T (2014) Celsr1 is required for the generation of polarity at multiple levels of the mouse oviduct. *Development* **141**: 4558-4568.
2. Shirayoshi Y, Nose A, Iwasaki K, Takeichi M (1986) N-Linked Oligosaccharides Are Not Involved in the Function of a Cell-Cell Binding Glycoprotein E-Cadherin. *Cell Structure and Function* **11**: 245-252
3. Matsumoto S, Fumoto K, Okamoto T, Kaibuchi K, Kikuchi A (2010) Binding of APC and dishevelled mediates Wnt5a-regulated focal adhesion dynamics in migrating cells. *EMBO J* **29**: 1192-1204
4. Metzger T, Gache V, Xu M, Cadot B, Folker ES, Richardson BE, Gomes ER, Baylies MK (2012) MAP and kinesin-dependent nuclear positioning is required for skeletal muscle function. *Nature* **484**: 120-124